Searching for fast optical transients with Mini-MegaTORTORA wide-field monitoring system

S. Karpov[1,3],*, G. Beskin[1,3], A. Biryukov[3,4], S. Bondar[2], E. Ivanov[2], E. Katkova[2], N. Orekhova[2], A. Perkov[2], V. Plokhotnichenko[1], V. Sasyuk[3], J. Pandey[5]

[1]Special Astrophysical Observatory of Russian Academy of Sciences, Russia; karpov.sv@gmail.com

[2]Research and Production Corporation "Precision Systems and Instruments", Russia

[3]Kazan Federal University, Russia

[4]Moscow State University, Russia

[5]Aryabhatta Research Institute of Observational Sciences (ARIES), Nainital-263002, India

Abstract Here we present the summary of first years of operation and the first results of a novel 9-channel wide-field optical monitoring system with sub-second temporal resolution, Mini-MegaTORTORA (MMT-9), which is in operation now at Special Astrophysical Observatory on Russian Caucasus. The system is able to observe the sky simultaneously in either wide (~900 square degrees) or narrow (~100 square degrees) fields of view, either in clear light or with any combination of color (Johnson-Cousins B, V or R) and polarimetric filters installed, with exposure times ranging from 0.1 s to hundreds of seconds. The real-time system data analysis pipeline performs automatic detection of rapid transient events, both near-Earth and extragalactic. The objects routinely detected by MMT include faint meteors and artificial satellites.

Keywords: telescopes — instrumentation: miscellaneous — gamma-ray burst: general — meteorites, meteors, meteoroids

1. Introduction

Mini-MegaTORTORA is a novel robotic instrument just commissioned for the Kazan Federal University and developed according to the principles of MegaTORTORA multi-channel and transforming design formulated by us earlier [1]-[4],[24],[25]. It is a successor to the FAVOR [5]-[7] and TORTORA [8] single-objective monitoring instruments we built earlier to detect and characterize fast optical transients of various origins, both cosmological, galactic and near-Earth. The importance of such instruments became evident after the discovery and detailed study of the brightest ever optical afterglow of a gamma-ray burst, GRB080319B [9],[10].

The Mini-MegaTORTORA (MMT-9) system includes a set of nine individual channels (see ***Fig1***) installed in pairs on equatorial mounts (see ***Fig2***). Every channel has a celostate mirror installed before the Canon EF85/1.2 objective for a rapid (faster than 1 second) adjusting of the objective direction in a limited range (approximately 10 degrees to any direction). This allows for either mosaicking the larger field of view, or for pointing all the channels in one direction. In the latter regime, a set of color (Johnson's B, V or R) and polarimetric (three different

directions) filters may be inserted before the objective to maximize the information acquired for the observed region of the sky (performing both three-color photometry and polarimetry).

The channels are equipped with an Andor Neo sCMOS detectors having 2560x2160 pixels 6.4μm each. Field of view of a channel is roughly 9x11 degrees with angular resolution of 16″ per pixel. The detector is able to operate with exposure times as small as 0.03 s, in our work we use 0.1 s exposures providing us with 10 frames per second as on higher frame rates we are unable to process the data in real time.

Every channel is operated by a dedicated PC which controls its hardware, acquires the images from the detector and performs the data processing. The amount of data acquired by a single channel is about 3Tb in 8 hours of observations. The complex as a whole is being controlled by a separate PC.

Initial tests show that the FWHM of the stars as seen by MMT channels is around 2 pixels wide. The detection limit in white light for 0.1 s exposure is close to 11 mag, when calibrating to V band magnitudes.

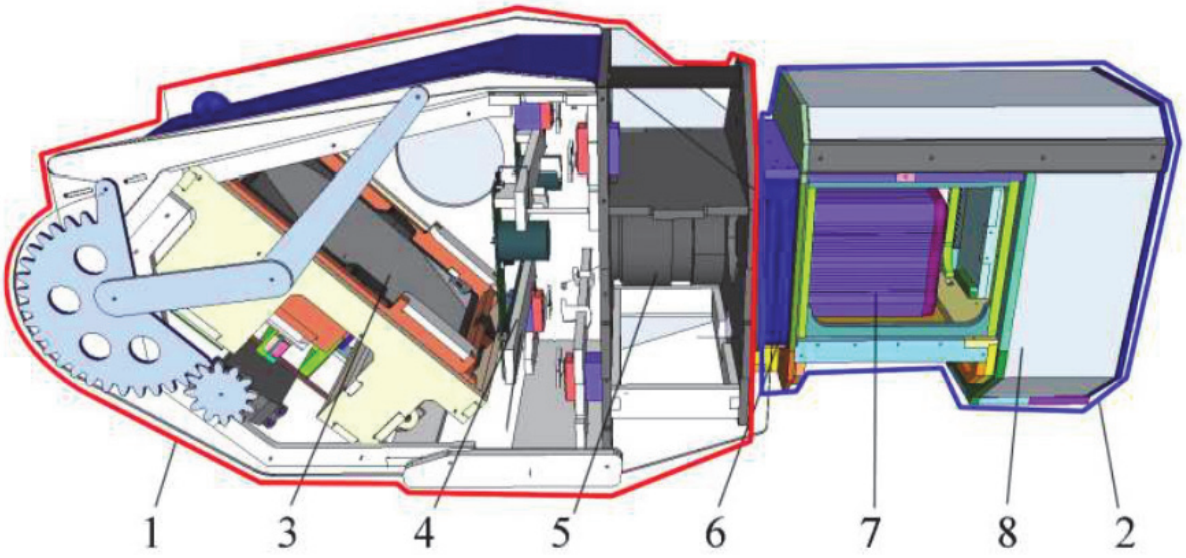

Fig1. *Schematic view of a MMT channel. 1 – celostate unit, 2 – camera unit, 3 – celostate mirror which can rotate for ~ 10 degrees around two axes, 4 – installable color and polarimetric filters, 5 – Canon EF85/1.2 objective, 6 – optical corrector, 7 – Andor Neo sCMOS detector, 8 – conditioner to keep stable environmental conditions inside the channel.*

2. Mini-MegaTORTORA operation

Mini-MegaTORTORA started its operation in June 2014, and routinely monitor the sky since then. The observations are governed by the dedicated dynamic scheduler optimized for performing the sky survey. The scheduler works by selecting the next pointing for Mini-MegaTORTORA by simultaneously optimizing the following parameters: distances from the Sun, Moon and the horizon should be maximized, distances from the current pointings of Swift and Fermi satellites should be minimized, and the number of frames already acquired on a given sky position that night should be minimized. In this way more or less uniform survey of the whole sky hemisphere is being performed while maximizing the probability of observations of gamma-ray bursts. As an unoptimized extension, the scheduler also supports the observations of pre-selected targets given by their coordinates, which may be performed in various regimes

Fig2. *Photo of the all 9 channels of MMT installed on 5 mounts in the single cylindrical dome, which is open at that moment. Russian 6-m telescope may be seen in the background.*

supported by Mini-MegaTORTORA (wide-field monitoring of a given region of the sky with or without filters, narrow-field multicolor imaging or polarimetry with lower temporal resolution, etc).

2.1. Real-time transient detection

The main regime of Mini-MegaTORTORA operation is the wide-field monitoring with high temporal resolution and with no photometric filters installed. In this regime, every channel acquires 10 frames per second, which corresponds to 110 megabytes of data per second. To analyze it, we implemented the real-time fast differential imaging pipeline intended for the detection of rapidly varying or moving transient objects – flashes, meteor trails, satellite passes etc. It is analogous to the pipeline of FAVOR and TORTORA cameras [11],[7], and is based on building an iteratively-updated comparison image of current field of view using numerically efficient running median algorithm, as well as threshold image using running similarly constructed *median absolute deviation* estimate, and then comparison of every new frame with them, extracting candidate transient objects and analyzing lists of these objects from the consecutive frames. It then filters out noise events, extracts the meteor trails by their generally elongated shape on a single frame, collects the events corresponding to moving objects into focal plane trajectories, etc. Data on detected transients are stored to the database and are partially published online [1].

Every 100 frames acquired by a channel are being summed together, yielding "average" frames with 10 s effective exposure and better detection limit. Using these frames, the astrometric calibration is being performed using locally installed ASTROMETRY.NET code [12]. Also the rough photometric calibration is being done. These calibrations, updated every 10

1 Public databases of meteors [15] and artificial satellites [16] observed by Mini-MegaTORTORA are available at project website at http://mmt.favor2.info

seconds, are used for measuring the positions and magnitudes of transients detected by the real-time differential imaging pipeline. The "average" frames are stored permanently (in contrast to "raw" full-resolution data which is typically erased in a day or two after acquisition) and may be used later for studying the variability on time scales longer than 10 s.

The Mini-MegaTORTORA typically observes every sky field continuously for 1000 seconds before moving to the next pointing. Before and after observing the field with high temporal resolution, the system acquires deeper "survey" images with 60 seconds exposure in white light in order to study the variability of objects down to 14-15 magnitude on even longer time scales; typically, every point of the northern sky is covered by one or more such images every observational night.

Mini-MegaTORTORA real-time transient detection system routinely extracts various kinds of transient from the data stream – rapid flashes, meteors, satellites etc.

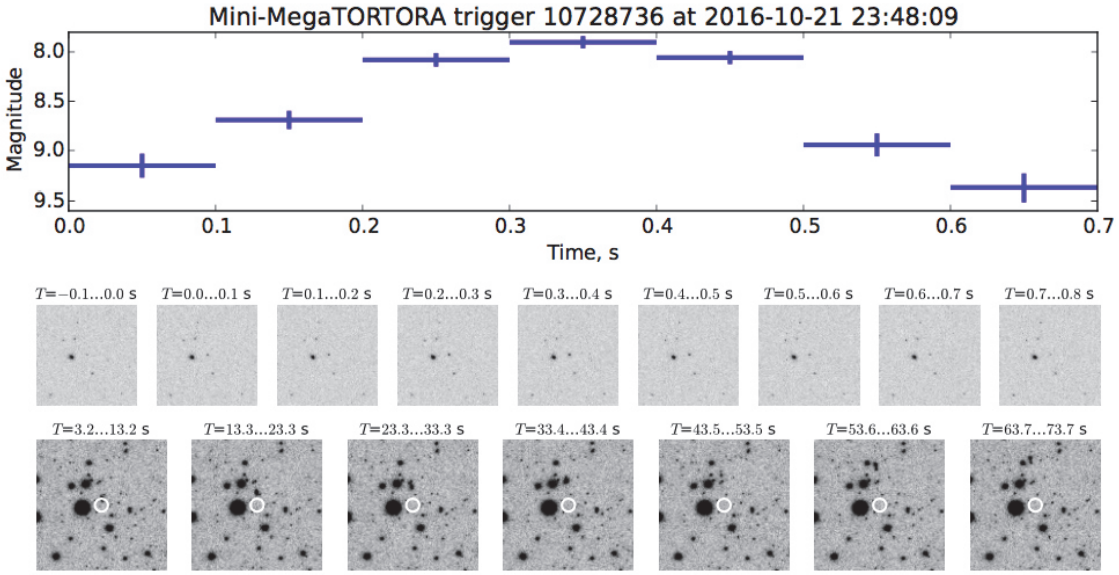

***Fig3**. Example of a rapid optical flash independently detected and followed-up by Mini-MegaTORTORA and not identified with satellites from NORAD database. Upper panel – light curve with 0.1 s temporal resolution, middle panel – corresponding detection images (50' x 50' around the event), lower panel – follow-up images with 10 s exposures that clearly reveal a satellite slowly moving away from the flash position.*

The rapid flashes – i.e. the optical transients rapidly changing their brightness and not displaying signs of motion – are then matched against stellar catalogues to exclude events due to stellar scintillations, and against public NORAD database of satellite orbits [13] to filter out satellite flashes. All the remaining flashes have the same characteristic properties – durations, shapes, peak magnitudes (see ***Fig4***) – as the ones caused by identified satellites, and we may suggest that they are also due to satellites, but either missing from public database of orbits, or having quite large errors in their orbital parameters. Moreover, immediate follow-up observations using Mini-MegaTORTORA rapid reaction mode (see ***Fig3*** for a typical example) often reveal faint satellite trails leading from the event location. Therefore we may conclude that no bright rapid flashes of astrophysical origin are detected in 2.5 years of Mini-MegaTORTORA operation.

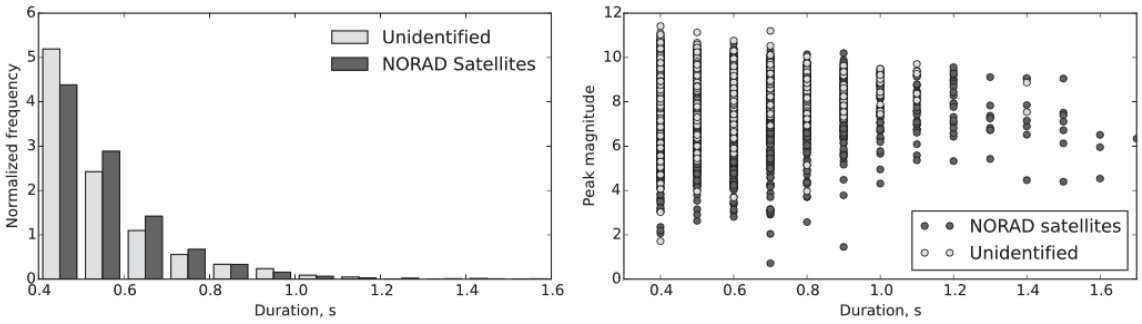

***Fig4**. Comparison of durations (left panel) and brightness (right panel) of rapid flashes detected by Mini-MegaTORTORA and identified/non-indentified with NORAD satellites.*

2.2. Follow-up observations of external triggers

Mini-MegaTORTORA also performs follow-up of Swift, Fermi and LIGO-Virgo triggers. Its large field of view, allowing for simultaneous observations of ~900 sq.deg. sky regions, makes it the perfect instrument for following up events with poor localization accuracy. On the other hand, the triggers with better localizations may be observed in multicolor and/or polarimetric regimes simultaneously.

Since mid-2015, 4 of 89 Swift GRBs have been followed up in narrow-field polarimetric mode in 30 to 60 seconds since trigger distribution through GCN network, with no optical emission detections. 9 of 250 Fermi GBM triggers have been also followed up in wide-field mode in 20 to 90 seconds from the trigger. All other events were either below the horizon or occurred in bad weather conditions.

2.3. Simultaneous observations of Fermi GRB151107B

The localization of Fermi GBM trigger GRB151107B [17],[18] has been observed before, during and just after the trigger time, covering nearly all its error box (see ***Fig5***) simultaneously since T-329.3 s till T+25.7 (including brightest part of first gamma-ray peak) with temporal resolution of 0.1 s in white light. Dedicated real-time transient detection pipeline did not detect any events longer than 0.3 s and brighter than approximately V=10.5 mag. Inspection of co-added images with 10 s effective exposure has not revealed any variable source down to V=12.0 mag during that interval.

After receiving GCN trigger the system initiated a wide-field follow-up and since T+62.7 s (during the continuing gamma-ray activity) till T+666.7 s acquired 20x9 deep images with 30 s exposures in a 30x30 degree field of view covering the whole final 1-sigma localization box. Analysis of the acquired data has not revealed any variable object down to roughly V=13.5 mag over the time interval [18].

3. Detection of the optical counterpart of Fermi GRB 160625B

One more Fermi event, GRB 160625B, has been followed up in the widefield regime, with bright optical flash of GRB 160625B clearly detected during the gamma activity [19].

The on-sky position of the Fermi gamma-ray burst GRB 160625B has been observed before, during and just after the LAT trigger time (T = 2016-06-25 22:43:24). Mini-MegaTORTORA reacted to the Fermi GBM trigger no. 488587220 generated as a result of the detection of the precursor and started observing its error box 52 seconds after it and 136 seconds before LAT trigger. Due to large size of GBM error box, the observations have been performed in “wide-

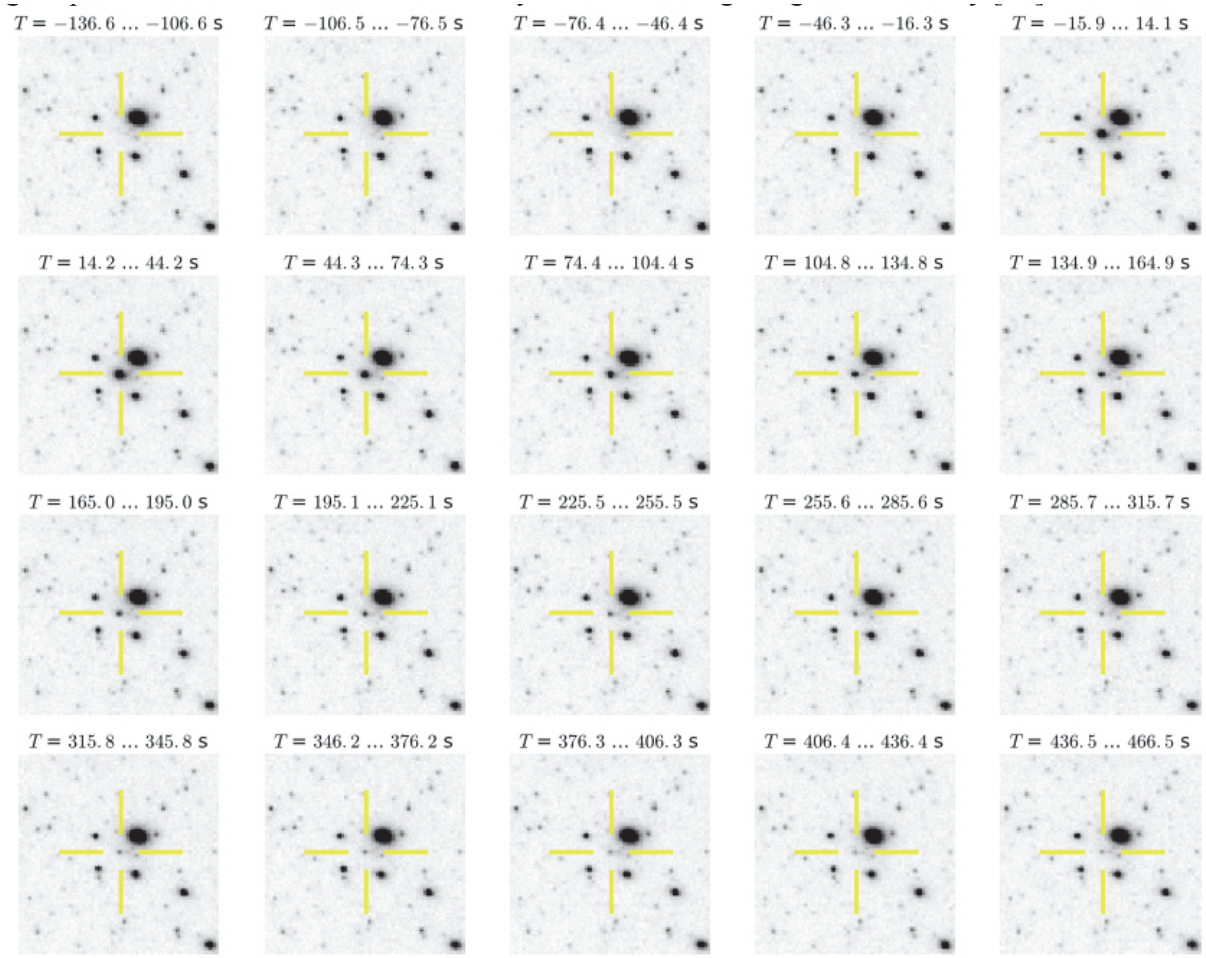

Fig 5*. The final localization region of GRB 160625B as seen by Mini-MegaTORTORA (20 unfiltered images with 30-s exposures). The peak brightness of transient object is V=8.8 mag.*

field+deep" regime, with channels simultaneously covering 30x30 deg field of view (see ***Fig3***) with 30 s exposures in white light to achieve deepest detection limit. The system acquired 20 frames in such regime, covering time interval from T − 136 to T + 466 s, and detected a bright optical transient with a mag- nitude of about V = 8.8 mag on a frame coincident with LAT trigger time (T − 15.9 – T + 14.1 s) at the coordinates consistent with the afterglow [20]. On the consecutive frames, the transient brightened for about 0.1 mag, and then faded following nearly smooth power-law decay with slope of about −1.6, down to V = 12.2 at last acquired frame. The images acquired prior to LAT trigger do not display any object at that position down to about V = 13.5 mag. This sequence of frames (20′ subimages centered on the transient) is shown in ***Fig5.***

The system also responded to the second GBM trigger no. 488587880 with a somewhat different coordinates. This response resulted in the acquisition of 20 more frames covering burst position in the time interval from T + 1691 to T +2264 s. In this sample no transient objects brighter than V = 13.5 mag were detected.

The optical light curve shown in ***Fig6*** displays an initial peak with duration similar to the one of the gamma-ray peak and seemingly corresponding to the prompt phase of emission, gradually transforming into the afterglow about 50 s after the onset of the gamma-ray event. Such a behavior – the absence of the intensity dip between the prompt optical emission

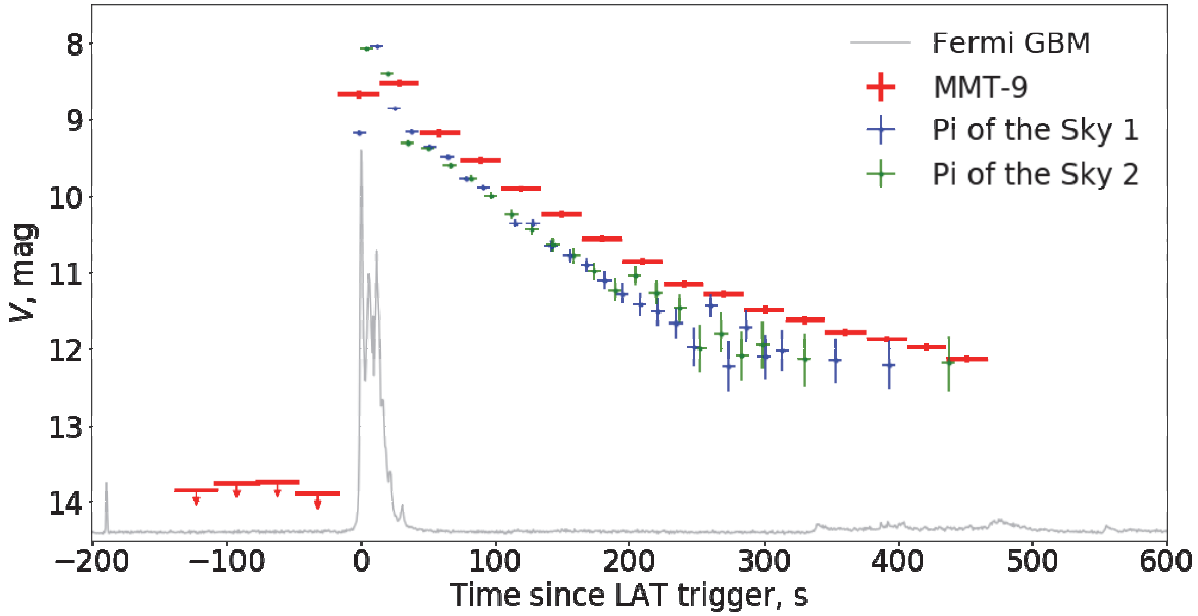

Fig.6. *The light curve of optical transient that accompanied the second gamma activity episode of GRB 160625B, as seen by Mini-MegaTORTORA. Also, the data acquired by Pi~of~the~Sky cameras [22] are shown.*

accompanying the gamma-ray burst and the afterglow – is typical for several most powerful bursts including GRB 080319B (Naked-Eye Burst) [9]. This is not the only similarity between these two events. Indeed, in both cases the intensity of the optical emission accompanying the gamma-ray burst exceeds the extrapolation of the gamma-ray spectrum to the optical range, which indicates different generation mechanisms of these two emission components. Moreover, gamma-ray peaks precede the corresponding optical flashes in time. Indeed, a comparison of the light curves of GRB 160625B in different spectral intervals (see ***Fig6*** where we used both the Mini-MegaTORTORA data and the results obtained by Pi of the Sky wide-field monitoring system [22]) shows that optical and gamma-ray emission in the second activity episode are correlated, and the latter precedes the optical flash by 2–4 s. Given the measured redshift of the object, which was found to be close to 1.4 [21], we find that in the comoving frame optical emission lags behind gamma-ray emission for 1–2 s, like in the Naked-Eye Burst where the same lag was found. We may conclude that in both cases optical photons are born 10–100 times farther away from the "central engine" than high-energy photons, i.e., in jet regions that are spaced apart [9], and that in the GRB 160625B electrons are heated by internal shocks originating from the residual collisions of filaments ejected in the jet, and the observed emission is generated by their synchrotron energy release [23].

4. Photometric analysis of Mini-MegaTORTORA data

Most of the Mini-MegaTORTORA observational time since its commissioning in mid-2014 is dedicated to the high temporal resolution (with exposure of 0.1 s and limit of about V=11 mag) wide-field monitoring of the sky in order to detect and classify rapid optical transients in real time, and to perform their follow-up. In addition to this "monitoring" operation, the system performs deeper "survey" imaging of the sky (one to few frames per night per field with 20 to 60 s exposure and limit down to V=14.5 mag; more than 300000 frames to date). Moreover, during the monitoring, intermediate depth "running sums" images with 10 s effective exposures (limit of about V=12.5 mag), amounting typically for 100 consecutive images, spanning 1000 seconds in total, per field, are generated and stored.

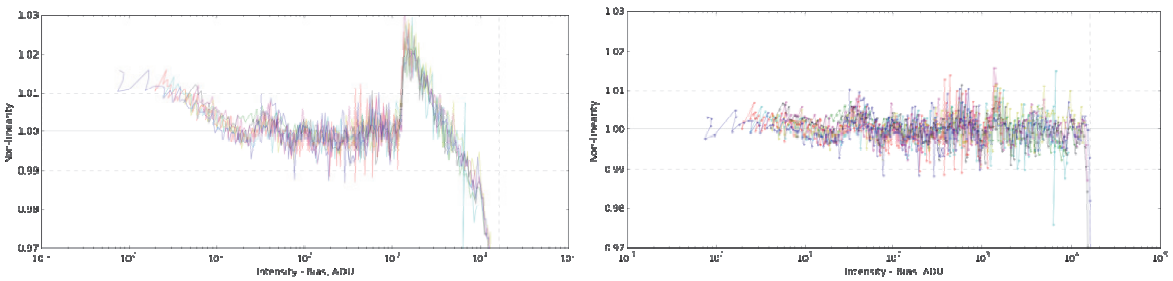

Fig7. *Left – non-linearity of Andor Neo sCMOS detector in global shutter mode as a function of intensity due to its dual-amplifier design. Right – the same after applying linearization correction defined as a piecewise fourth-order polynomial with parameters calibrated on a per-pixel basis.*

Mini-MegaTORTORA has not been originally designed to be a precise photometric instrument, as it uses fast but less reliable Andor Neo sCMOS detectors in place of more typical and accurate CCDs. Due to it, precise calibration of imaging data from Mini-MegaTORTORA requires thorough study of peculiarities, non-linearity (see ***Fig7***) and stability of its detectors, which is now ongoing.

In general, the archive of Mini-MegaTORTORA images represents a time-domain picture of the sky on time scales ranging from tens of seconds to years, with hundreds to tens of thousands points for every object, and in principle allows to extract and characterize the majority of variable objects down to V=14.5 mag. Examples of data extracted from the archive for different classes of variable objects are shown in ***Figs 8,9,10.***

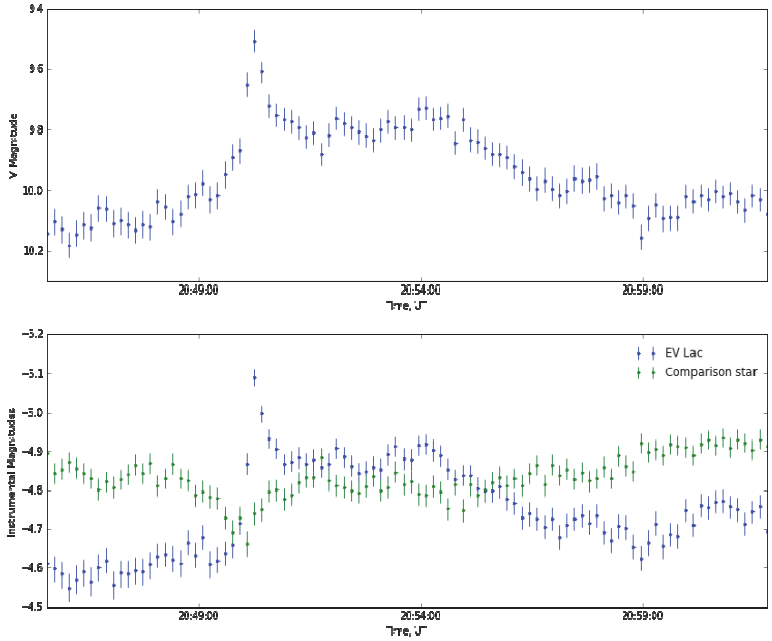

Fig8. *Light curve of EV Lac flaring star extracted from "running sum" frames (10 s effective exposure, derived by averaging 100 consecutive frames acquired in monitoring) in Mini-MegaTORTORA archive. The unfiltered instrumental magnitudes (lower panel) are calibrated to V band (upper panel) by using the comparison star of similar color to the object. The noise in the frames is estimated as a spatial variance and is mostly due to sCMOS non-uniform bias map. Instrumental magnitudes demonstrate temporally correlated trents due to drifting of pixel bias values and slow motion of the stars over different pixels due to imperfect tracking.*

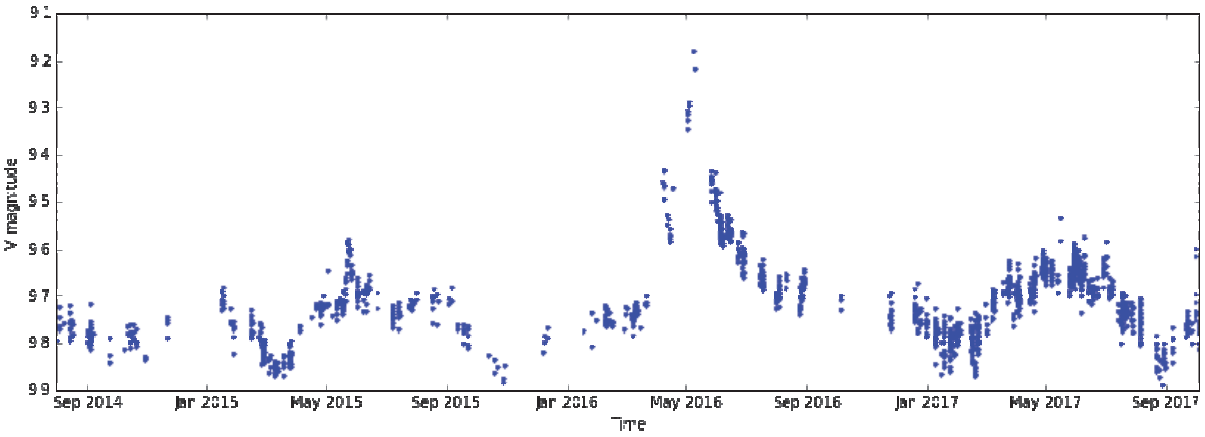

Fig9. *Light curve of AG Dra symbiotic binary star extracted from "survey" images stored in Mini-MegaTORTORA data archive. The large outburst around May 2016 is clearly visible, along with some smaller ones before and after.*

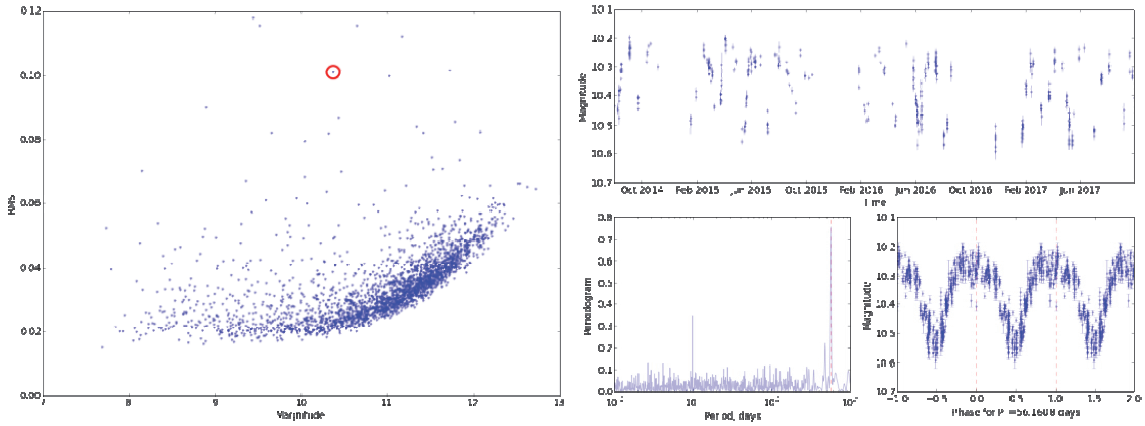

Fig10. *New variable star detected in the Mini-MegaTORTORA data. Left – scatter vs mean magnitude plot with the star marked by a red circle. Right – light curve, periodogram and a folded light curve corresponding to the best period detected in periodigram for the star.*

Acknowledgements

This work was supported by the grant of RFBR No.17-52-45048. Mini-MegaTORTORA belongs to Kazan Federal University and the work is performed according to the Russian Government Program of Competitive Growth of Kazan Federal University. Observations on Mini-MegaTORTORA are supported by the Russian Science Foundation grant No. 14-50-00043.

References

[1] Beskin, G., Bondar, S., Karpov, S., Plokhotnichenko, V., Guarnieri, A., Bartolini, C., Greco, G., Piccioni, A., & Shearer, A. 2010a, Advances in Astronomy, 2010

[2] Beskin, G. M., Karpov, S. V., Plokhotnichenko, V. L., Bondar, S. F., Perkov, A. V., Ivanov, E. A., Katkova, E. V., Sasyuk, V. V., & Shearer, A. 2013, Physics Uspekhi, 56, 836

[3] Beskin, G., Karpov, S., Bondar, S., Perkov, A., Ivanov, E., Katkova, E., Sasyuk, V., Biryukov, A., & Shearer, A. 2014, in Revista Mexicana de Astronomia y Astrofisica Conference Series, Vol. 45, Revista Mexicana de Astronomia y Astrofisica Conference Series, 20

[4] Biryukov, A., Beskin, G., Karpov, S., Bondar, S., Ivanov, E., Katkova, E., Perkov, A., & Sasyuk, V. 2015, Baltic Astronomy, 24, 100

[5] Zolotukhin, I., Beskin, G., Biryukov, A., Bondar, S., Hurley, K., Ivanov, E., Karpov, S., Katkova, E., & Pozanenko, A. 2004, Astronomische Nachrichten, 325, 675

[6] Karpov, S., Beskin, G., Biryukov, A., Bondar, S., Hurley, K., Ivanov, E., Katkova, E., Pozanenko, A., & Zolotukhin, I. 2005, Nuovo Cimento C, 28, 747

[7] Karpov, S., Beskin, G., Bondar, S., Guarnieri, A., Bartolini, C., Greco, G., & Piccioni, A. 2010, Advances in Astronomy, 2010

[8] Molinari, E., Bondar, S., Karpov, S., Beskin, G., Biryukov, A., Ivanov, E., Bartolini, C., Greco, G., Guarnieri, A., Piccioni, A., Terra, F., Nanni, D., Chincarini, G., Zerbi, F., Covino, S., Testa, V., Tosti, G., Vitali, F., Antonelli, L., Conconi, P., Malaspina, G., Nicastro, L., & Palazzi, E. 2006, Nuovo Cimento B, 121, 1525

[9] Beskin, G., Karpov, S., Bondar, S., Greco, G., Guarnieri, A., Bartolini, C., & Piccioni, A. 2010b, ApJ, 719, L10

[10] Beskin, G. M., Karpov, S. V., Bondar, S. F., Plokhotnichenko, V. L., Guarnieri, A., Bartolini, C., Greco,G., & Piccioni, A. 2010c, Physics Uspekhi, 53, 406

[11] Beskin, G., Biryukov, A., Bondar, S., Hurley, K., Ivanov, E., Karpov, S., Katkova, E., Pozanenko, A., & Zolotukhin, I. 2004, Astronomische Nachrichten, 325, 676

[12] Lang, D., Hogg, D. W., Mierle, K., Blanton, M., & Roweis, S. 2010, AJ, 139, 1782

[13] US Department of Defence. 2015, Database of satellite orbital parameters, available at http://www.space-track.org/

[14] McCants, M. 2015, Satellite Tracking TLE page, available at https://www.prismnet.com/~mccants/tles/index.html

[15] Karpov, S., Katkova, E., Beskin, G., et al. 2016b, Revista Mexicana de Astronomia y Astrofisica Conference Series, Vol. 48, 112–113

[16] Karpov, S., Orekhova, N., Beskin, G., et al. 2016c, Revista Mexicana de Astronomia y Astrofisica Conference Series, Vol. 48, 97–98

[17] Stanbro, M. & Meegan, C. 2015, GRB Coordinates Network, 18570

[18] Karpov, S., Beskin, G., Bondar, S., et al. 2015, GRB Coordinates Network, 18574

[19] Karpov, S., Beskin, G., Bondar, S., et al. 2016a, GRB Coordinates Network, 19603

[20] Troja, E., Butler, N., Watson, A. M., et al. 2016, GRB Coordinates Network, 19588

[21] Xu, D., Malesani, D., Fynbo, J. P. U., et al. 2016, GRB Coordinates Network, 19600

[22] Batsch, T., Castro-Tirado, A. J., Czyrkowski, H., et al. 2016, GRB Coordinates Network, 19615

[23] Li, Z. & Waxman, E. 2008, ApJ, 674, 65

[24] Beskin, G., Karpov, S., Biryukov, A. et al. 2017, Astrophysical Bulletin, Volume 72, Issue 1, pp.81-92

[25] Karpov, S., Beskin, G., Biryukov, A. et al. 2016, Revista Mexicana de Astronomía y Astrofísica (Serie de Conferencias) Vol. 48, pp. 91-96